STATIC STABILITY

J A Young, University of Wisconsin, Madison, WI, USA

Introduction

Static stability measures the gravitational resistance of an atmosphere to vertical displacements. It results from fundamental buoyant adjustments, and so it is determined by the vertical stratification of density or potential temperature. It influences the dynamics of many kinds of atmospheric motions, which in turn are responsible for determining its variations.

Static stability is represented commonly by the square of the buoyancy frequency N, which plays a role in theories for flow instabilities, wave propagation, and forced motions. As summarized below, these theories apply to a wide range of spatial scales, from small-scale turbulence to convection, mesoscale motions, and large-scale circulations for which the ratio of N to the Coriolis frequency f is paramount.

Basic Buoyant Stability and Instability

The role of density fluctuations in a gravity field is best in the vertical component of the equations of motion. In an absolute sense, the gravity and pressure gradient forces are usually in a state of hydrostatic balance to within 1%. However, the slight imbalances account for vertical accelerations $\mathrm{d}w/\mathrm{d}t$ which are often driven by buoyancy:

$$\mathrm{d}w/\mathrm{d}t = -\rho_0^{-1}[\mathrm{d}p'/\mathrm{d}z] + B \qquad [1]$$

Here, w is the vertical velocity $\mathrm{d}z/\mathrm{d}t$, t is the time, $\rho_0(z)$ is the density of a static 'environmental' reference state, and a prime indicates deviation from that reference state. B is the buoyancy force per unit mass, given by $B = -\rho'/\rho_0 g$. For many buoyant motions, B is an upper bound on vertical accelerations $\mathrm{d}w/\mathrm{d}t$ since the pressure gradient term tends to oppose B. The most useful approximate form for B is

$$B = (\theta_v'/\theta_{v0})g \qquad [2]$$

where θ_v is the potential temperature augmented by a small (at most, a few °C) amount proportional to water vapor, reflecting the contribution of humidity fluctuations to buoyancy.

For a dry adiabatic vertical displacement δz, a parcel conserves θ_v so that $\theta_v' = -(\partial\theta_{v0}/\partial z)\delta z$. For a stable system, the squared frequency of oscillation is commonly equal to the restoring force per displacement, or $B/\delta z$ in this case. Thus, if pressure effects are ignored in eqn [1], the simple buoyancy frequency N is given by

$$N^2 = (g/\theta_{v0})\partial\theta_{v0}/\partial z \qquad [3]$$

N, also known as the Brunt–Vaisalla frequency, is determined by the vertical gradient of θ_{v0} or equivalently by the difference between virtual temperature lapse rate $-\partial T_v/\partial z$ and the dry adiabatic rate $\Gamma_d = g/cp$. Unless conditions are superadiabatic, θ_{v0} increases upward, corresponding to static stability. In this case, N^2 is positive and eqns [1]–[3] imply

$$\mathrm{d}^2w/\mathrm{d}t^2 + N^2w = 0 \qquad [4]$$

It follows that the solution is a simple oscillation $w(t) = W\cos(Nt + \varepsilon)$, where W is the maximum vertical velocity amplitude and ε is a phase constant. The period is $2\pi/N$, typically about 10 min in the troposphere. **Figure 1A** shows the vertical oscillation, and its driving by buoyancy, which is a quarter cycle ahead of the parcel displacement δz. The buoyancy oscillation is analogous to that of a spring, so N^2 is equivalent to the 'stiffness' of the atmosphere when it is subjected to vertical displacements. The stiffness increases with the closeness of θ surfaces. **Figure 1B** shows that a larger stability produces a faster oscillation and inhibits the maximum vertical displacements W/N.

For smaller values of static stability, the restoring buoyancy forces are weaker and the oscillations are slower. Neutral stability occurs when $\partial\theta_{v0}/\partial z$ is zero (dry adiabatic conditions); a displaced parcel with no initial buoyancy remains that way, so there is no vertical acceleration. 'Absolute instability' occurs when $\partial\theta_{v0}/\partial z$ is further reduced to a negative value (superadiabatic lapse rate). In this case $N^2 = -|N^2|$ is negative, and the solutions to eqn [4] are exponential in time (**Figure 1C**). The growing mode ($\exp(|N|t)$) corresponds to a cooperative relation between buoyancy and motion (e.g., warm air rising) and may be thought of as the initial stage of convection. (A decaying mode ($\exp(-|N|t)$) corresponds to a mismatch of B and w (e.g., cold air rising) and so it is of no long-term consequence.) For convective motions, the increase of vertical kinetic energy is equal to the buoyancy work $\int B\,\delta z$, known as the convective available potential energy (CAPE) along the parcel's vertical path. (In vertically confined convective systems, a growing mode requires that thermal and viscous dissipation must be overcome, so a critical

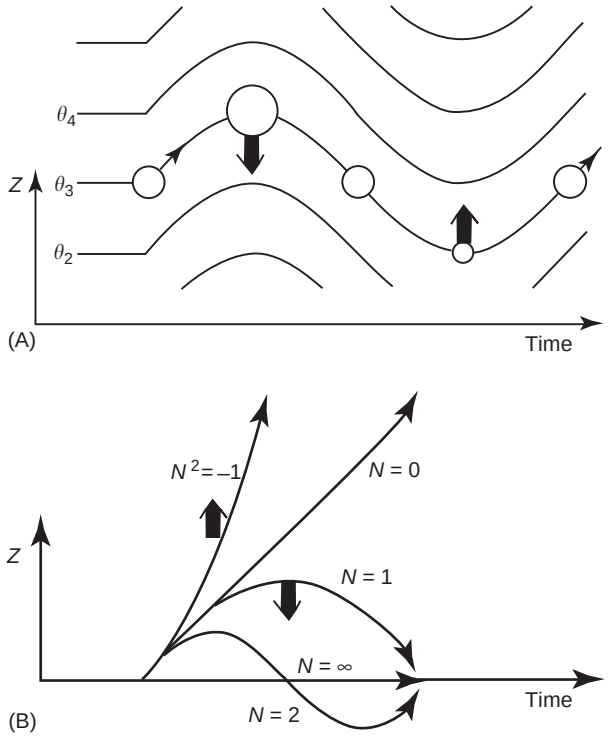

Figure 1 Simple buoyancy motions and varying environmental static stability. (A) Stable oscillation for $N = 1$. Isentropic surfaces are shown; increasing labels indicate warmer θ. Impulsive force creates initial vertical motion W (thin arrow), adiabatic displacements of θ surfaces, changes in air parcel volume (circles), and buoyancy force (vertical arrows). (B) Parcel motions for five stability conditions. Moderate stability: $N = 1$, shown in (A). Stronger stability: $N = 2$ stable oscillation has shorter period, smaller vertical displacements. Extreme stability: $N =$ infinity has no vertical displacement. Neutral stability: $N = 0$ has displacements growing linearly, with no restoring force. Unstable conditions: $N^2 = -1$ has buoyancy forces creating amplifying vertical parcel displacements.

value of $|N^2|$ must be exceeded, as expressed in a critical 'Rayleigh number' necessary for convection.) For many applications the distinction between θ and θ_v is of secondary importance, as is assumed in the remaining discussion.

Moist Instability

In a humid atmosphere, phase changes in the water content may cause instability even when N^2 is positive. In this case, a parcel conserves its equivalent potential temperature θ_e, rather than θ. θ_e exceeds θ by a temperature-dependent amount depending on humidity. As an example, conservation of θ_e is consistent with upward motions leading to saturation, the release of latent heat of condensation, and the diabatic increase of θ. These 'moist' diabatic processes reduce the effective static stability for cloud systems. For example, the stability of a cloud layer to internal displacements depends most strongly upon $\partial\theta_e/\partial z$, with negative values corresponding typically to instability. (This criterion is used to describe 'potential instability', an often-misused concept that describes the stability of an unsaturated layer which is lifted hypothetically until it becomes a cloud layer.)

The most important example of moist processes affecting stability occurs when rising, saturated parcels in cumulus clouds penetrate a dry 'environmental' layer. In this case, 'conditional instability' may occur even when $\partial\theta_{v0}/\partial z$ is positive and the 'dry dynamics' of the environment are stable. This instability criterion may be expressed as $\partial\theta_{es}/\partial z < 0$, where θ_{es} is the saturation equivalent potential temperature, a known function of T and pressure p. This criterion is met if the virtual temperature lapse rate $-\partial T_v/\partial z$ exceeds the smaller moist adiabatic rate Γ_m. The result is that the unstable combination of positive buoyancy with a rising parcel occurs if a saturated parcel moves upward through a layer of air where N^2 is insufficiently positive. **Figure 2** illustrates the three fundamental types of stability for an atmosphere.

The growth of cumulus clouds is overestimated by this simple parcel reasoning, because updrafts require compensating subsidence of the environment. The resulting adiabatic warming decreases the relative buoyancy of the cloud. A simple 'slice' theory shows that the effective stability of the system is then increased for finite-sized clouds; it can be represented as a combination of the moist and dry static stabilities. Additional stabilizing influences are turbulent mixing of momentum and thermodynamic quantities between the cloud and the environment, and the effects of pressure adjustments.

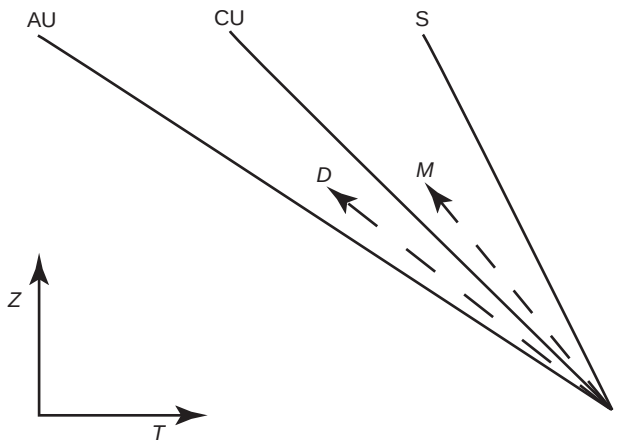

Figure 2 Vertical temperature profiles (solid) for three categories of static stability. Temperature changes for dry and moist adiabatic parcel displacements are dashed. AU: absolutely unstable; CU: conditionally unstable (for saturated parcels); S = absolutely stable.

Climatology of Static Stability

In the simplest terms, the dry and moist static stability indices depend upon vertical profiles of potential temperature, and to a lesser extent on the profile of water vapor. **Figure 3** shows some typical features in a vertical cross-section. Strong static stability (N^2) regions are associated with isentropic surfaces that are closely spaced in the vertical, a symptom of the vertical 'stiffness'. Weak stability regions have greater spacing, and the limit of zero stability may correspond to a vertical orientation of the isentropic surface. Regions of moist unstable motions are possible where there is a conditionally unstable temperature profile and sufficient moisture supply (e.g., the tropical boundary layer).

The distribution of static stability $\partial\theta/\partial z$ can be explained first by considering the processes that change the spacing Δz of potential temperature surfaces. From the first law of thermodynamics, it is easily shown that local changes of stability are caused by (1) advection of stability from upwind, (2) (vertically) differential temperature advection, and (3) differential diabatic heating. The differential diabatic term (3) explains many basic stability features in the atmosphere. The term is proportional to dJ/dz, where J is the diabatic heating rate per unit mass; negative J connotes cooling. This term increases the stability where J increases with height, and decreases it where J decreases with height.

Examples of diabatic influence on static stability are seen in **Figure 3**. The strongest stability is seen in the stratosphere, where stability is maintained by the radiative heating increase due to absorption of solar ultraviolet radiation by ozone. The tropospheric static stability is several times smaller, due especially to downward long-wave radiation. Near the Earth's surface, strong stability at high latitudes is created by long-wave radiative cooling, while weaker stability at other latitudes is driven by sensible heat from the surface. The sensible heating is concentrated in the atmospheric boundary layer, which often resembles a

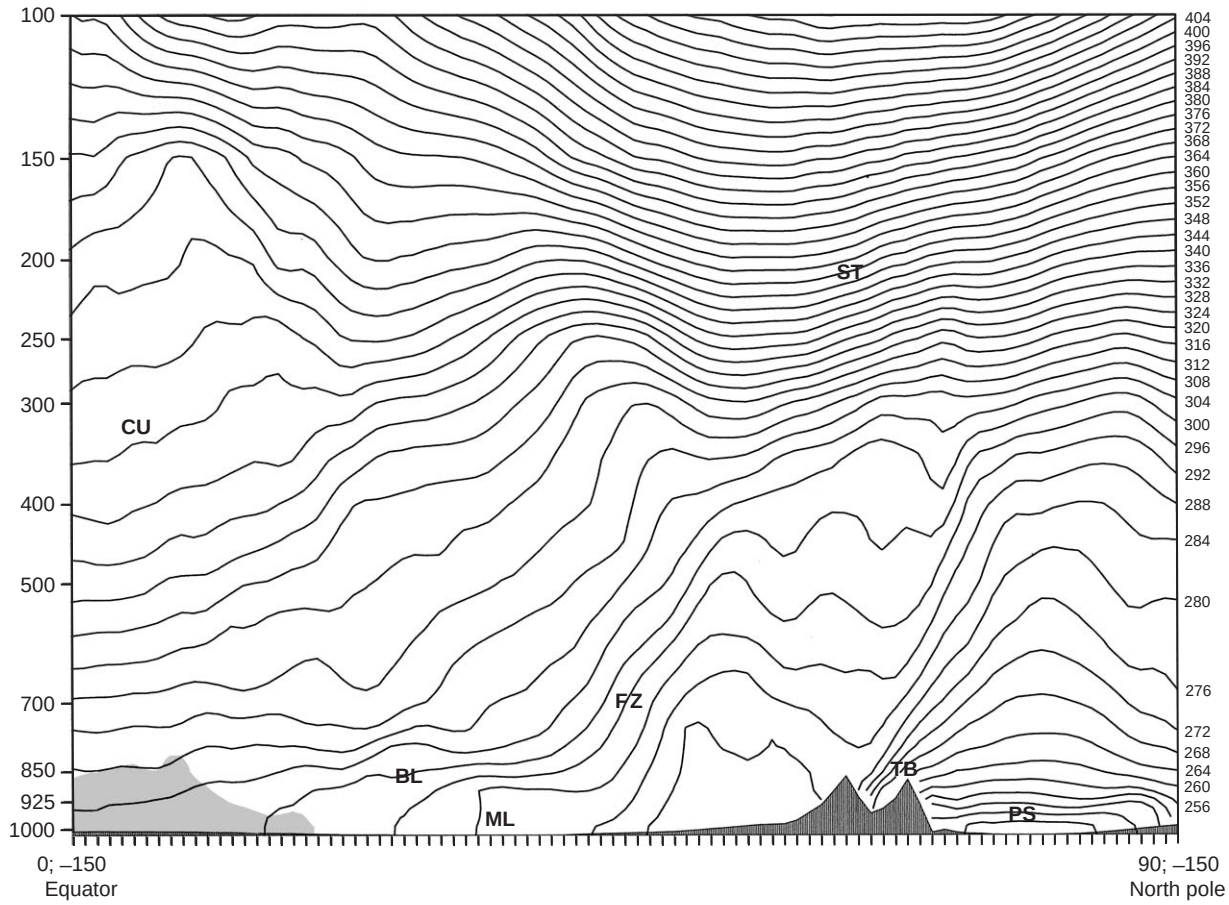

Figure 3 Vertical cross-section of θ from Equator to pole. Static stability is indicated by vertical closeness of θ surfaces. Left scale is pressure in hPa. Dark shading: Earth's topography. Light shading: boundary layer air with moisture mixing ratio exceeding 12 g kg^{-1}. Strong stability cases: ST – stratosphere, PS – polar surface, BL – boundary layer top, FZ – frontal zone, TB – topographic blocking by mountains. Weak stability: CU – conditionally unstable tropical troposphere, ML – convectively mixed boundary layer.

'convective mixed layer' of low stability, especially over land. In the tropics, the troposphere is moist at low levels, conditionally unstable, and deep; heavy cumulus convection is prevalent and its latent heating is the essential driving of the tropical climate system.

Some of the smaller-scale features in the figure are affected by adiabatic circulation processes. Term 2 includes the effect of vertical wind shear in a baroclinic region; near the Earth's surface, warm (cold) advection situations are associated commonly with stabilization (destabilization) of the lower atmosphere by this process. This term also explains the development of strong static stability by subsidence at the top of the atmospheric boundary layer and in frontal zones.

There are seasonal and diurnal variations in stability that cannot be represented in the snapshot (**Figure 3**). These variations are caused by those of solar radiative forcing of the Earth's surface, which results in variations of sensible and latent heating. Broadly speaking, the static stability fields tend to shift poleward in the summer season, and Equatorward in the winter season. The destabilization of the lower atmosphere is a maximum over land on summer days, while it is a maximum over the midlatitude oceans in winter.

Static Stability and Circulation Dynamics

Static stability influences the motions of the atmosphere on a range of scales and may permit waves to connect distant regions. Simple vertical buoyancy concepts are not sufficient for understanding these effects. In reality, one must also consider the coupling to horizontal winds and the ways in which pressure links the motion of different air parcels. The spatial distributions of static stability and wind determine the outcomes, which range from flow instability to various kinds of wave propagation in the horizontal and vertical.

Small-Scale Turbulence

Turbulence in the atmosphere may be caused by convection or by wind shear, and static stability is influential in each case. Ignoring moist dynamics, convection requires $\partial\theta_v/\partial z$ to be negative, which occurs most commonly when the air is in contact with a warmer Earth's surface, such as a sunny day over dry land. In such cases, N^2 is strongly negative in the surface layer (roughly the lowest 50 m), reflecting a superadiabatic lapse rate of virtual temperature. Static stability is then near-neutral ($N^2 = 0$) in a deeper 'mixed layer' up to the boundary layer top. Thus, neutral boundary layers are symptoms of surface-induced convection.

Positive static stability inhibits turbulence induced by wind shear. The production of shear turbulence may be understood by imagining a layer of concentrated wind shear which, when perturbed by vertical displacements, creates a pressure feedback that amplifies the displacements of the layer. The result is mixing of fast and slow air parcels by a growing pattern of Kelvin–Helmholtz instability (KHI) motions. Obviously, the vertical restoring forces of a statically stable atmosphere will oppose the vertical components of such KHI displacements. The competition between shear instability and stable stratification is best measured by the Richardson number

$$Ri = N^2/SH^2 \qquad [5]$$

where SH is most generally the magnitude of the vector wind shear $\partial\mathbf{V}/\partial z$. Ri is the squared ratio of the stable buoyancy oscillation frequency N to the maximum shear-induced growth rate SH. Theory and observation show that when $Ri > \frac{1}{4}$, shear growth is eliminated: static stability wins, and perturbations are stable oscillations as in **Figure 1**. On the other hand, when static stability is reduced so that $Ri < \frac{1}{4}$, the shear instability is not suppressed totally, and the perturbations may grow into turbulence.

In the free atmosphere, intense frontal zones are associated commonly with 'clear air turbulence', despite the zones having a maximum static stability. This is because they are sloping regions of strong gradients, and Ri is reduced more effectively by the strong shear as the vertical width of the zone becomes small. The mixing by this turbulence is thought to modify the mesoscale structure of the static stability and shear near jets.

Very near the Earth's surface, strong shear is created by frictional drag, but the turbulence is limited by the surface and by static stability. In such surface boundary layers, the intensity of shear turbulence is greatest beneath the height L, the Monin–Obukhov length. L varies inversely with the stable air–surface temperature difference and static stability near the ground. Higher in the boundary layer, the turbulent fluxes are often represented by eddy mixing coefficients which are a decreasing function of Ri (and hence static stability).

Mesoscale Motions

Static stability and its spatial variations may produce complex mesoscale motions. Since wind speeds and the frequencies of weather systems are strongly subsonic, it follows that the pressure fields are in a state of 'anelastic' balance with the temperature and velocity patterns. The simplest balance involving buoyancy B is described by the three-dimensional p.d.e.

$\nabla^2 p = \partial B/\partial z$, where ∇^2 is the elliptic Laplacian operator in three spatial dimensions. The buoyancy gradient term 'forces' a smooth pressure response which decreases inversely with distance. For a vertically oriented pattern of B, the pressure response is negligible, and simple buoyancy forces dominate the motion. However, a pattern of B tilted toward the horizontal produces a pressure gradient force that opposes B. Thus, static stability may be associated with motions that may or may not be in hydrostatic balance, depending on the distribution of buoyancy in the vertical plane.

The simplest tool for understanding these motions is the theory of buoyancy waves (*see* 'Atmospheric Waves'). For patterns of motion and temperature with phase fronts tilted at an angle α from the vertical, the free oscillation has a frequency $\omega = N \cos\alpha$. We see that N is actually an upper limit on the frequency, corresponding to the vertical orientation for a simple buoyancy oscillation. Such motions are nonhydrostatic. Much slower oscillations occur when the wave patterns are tilted toward the horizontal, a result of the 'braking' effect of the pressure field on the buoyant parcel. These motions are nearly hydrostatic, and the waves may propagate with a nondispersive phase speed obeying

$$c_G^2 = N^2/m^2 \qquad [6]$$

where m is the vertical wavenumber. Strong static stability corresponds to fast horizontal wave speeds.

There are dramatic consequences of the simple frequency dispersion relation. For example, the energy of the waves is transmitted along the sloping wave front at a group speed

$$c_g = N \sin\alpha/K \qquad [7]$$

where K is the two-dimensional wavenumber (inverse scale) of the wave pattern. We see that the energy propagation rate increases with static stability, and with angle α from the vertical. It follows that the response to a confined impulse will rapidly spread low-frequency energy horizontally, while higher frequencies will be found immediately above and below the region. Imposed frequencies greater than N are 'evanescent': such energy cannot be propagated away from the forcing. Interestingly, the orthogonal relation between phase and group velocity vectors implies that downward phase propagation is associated with upward energy propagation.

These properties have implications for a variety of mesoscale responses of a stable atmosphere to surface heating or mountains. For example, steady airflow U over a mountain complex may be envisioned in terms of periodic forcing. The above theory for low frequencies predicts that (1) a wide mountain may cause upwind 'blocking' of low-level air with high static stability, and (2) motions over the mountain are nearly in hydrostatic balance. The theory for higher frequencies suggests that very narrow mountains do not disturb the flow far above the mountain, but an intermediate mountain width yields a complex pattern of vertically propagating wave patterns extending upward and downwind of the mountain. In order for energy to propagate upward, the wave fronts must tilt upwind with increasing altitude and the waves transport wind momentum down into the mountain. An example is shown in **Figure 4**.

Static stability and wind variations influence the vertical fluxes of mesoscale wave energy and momentum which may link the upper atmosphere with the surface. For example, the vertical structure of the steady response with horizontal wavenumber k is governed by a propagation coefficient

$$P(z) = [N^2/U^2 - k^2] \qquad [8]$$

The wave profile 'propagates' vertically only when P is positive, or when static stability makes the Scorer parameter N^2/U^2 sufficiently large. The vertical wavenumber is then $P^{1/2}$. Variations in stability or wind will cause $P(z)$ to vary, which corresponds to

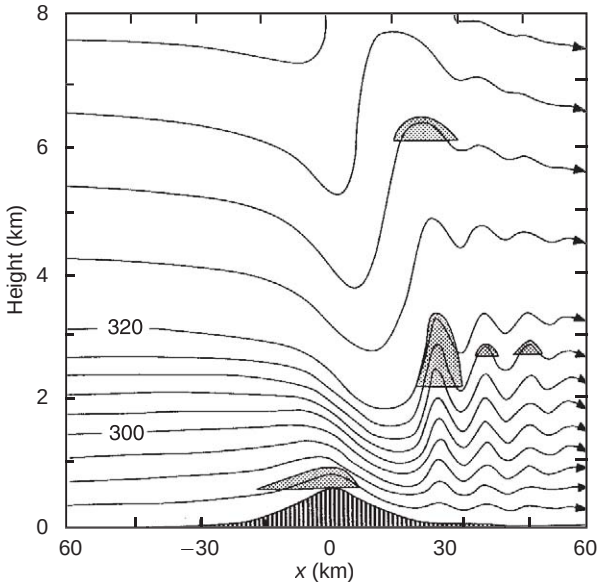

Figure 4 Streamlines and θ surfaces for flow over an isolated ridge. Upwind conditions have high static stability below 3 km, so $P(z)$ decreases upward. Wind speeds vary along streamlines in proportion to closeness of streamlines. Proceeding from the left, note the slowing of air on the upwind side, strong downslope wind, vertically tilted flow pattern, downwind jump, and lee waves trapped in the stable layer. Shading denotes possible clouds due to lifting of moist layers. (Reproduced with permission from Houze (1993, Figure 12.9). Courtesy of Dale Durran (1986).)

wave refraction in the vertical plane. Two categories of phenomena result, depending upon whether $P(z)$ decreases or increases with height.

If stability decreases with height, then $P(z)$ may become negative, and the wave may be reflected downward. Since the rigid Earth is also a reflecting surface for the wave vertical motion, the mountain-induced wave energy may become trapped in this layer. In this case, intense downslope winds and resonant 'lee' waves are possible. Other wave mechanisms, such as wave absorption at a critical layer where $U = 0$, depend more strongly on the wind profile.

In the other extreme, weak static stability in the boundary layer causes $P(z)$ to increase with height above the surface. A common idealization is a mixed layer ($N^2 = 0$) capped at height H by a sharp inversion of strength $\Delta\theta_v$. In this case, horizontal scales larger than H are hydrostatic and move with speeds of 'shallow water' gravity waves obeying

$$c_G^2 = [g'H] \qquad [9]$$

We see that $g' = g(\Delta\theta_v/\theta_v)$, the 'reduced gravity' parameter for the inversion, plays an analogous role to static stability for these hydrostatic motions. An example of this kind of motion is the propagation of a gust front, the leading edge of thunderstorm outflow in the boundary layer. Another example is where this kind of air layer is forced to flow over a mountain at speed U; the inversion stability appears inversely in the Froude number $F = U^2/(g'H)$. This number represents a competition between the flow inertia and the inversion stability, or equivalently between advection by U and gravity wave propagation c_G. Values exceeding O(1) may be associated with blocking on the upwind side of mountains, and strong downslope winds and hydraulic jumps on the downwind side.

Large-Scale Circulations

Large-scale circulations are those of large horizontal dimension, associated with low frequencies and hydrostatic balance. For such motions, static stability and the rotation of the Earth are important. Coriolis effects limit horizontal parcel motions in a fashion somewhat analogous to the buoyancy oscillation. The natural frequency of this 'inertia oscillation' is simply the Coriolis parameter f, which is about 100 times smaller than N. Thus, large-scale dynamics is ruled by the two fundamental frequencies of geophysical fluid dynamics: N and f. The most important large-scale flow variable is the combination known as the potential vorticity

$$q = (f + \varsigma)N^2 \qquad [10]$$

which is proportional to both the absolute vorticity of the winds and the static stability. Two frequency classes of large-scale waves are possible. The higher frequency class is inertio-gravity waves that obey

$$\omega^2 = f^2 + N^2(k^2/m^2) \qquad [11]$$

Static stability is seen to increase the minimum frequency f. These motions are never in a state of geostrophic balance, so they play an important role in the transient adjustments to thermal and mechanical forcing of the atmosphere. Vertical propagation of wave energy occurs only when frequency ω exceeds f. For example, diurnal atmospheric tides propagate vertically only Equatorward of 30° latitude.

Horizontal energy propagation is highly dispersive as a result of the Coriolis term: the largest scales propagate energy very slowly, while the smallest scales do so at the fast gravity wave speed c_G. The separation between large and small horizontal scales occurs at

$$\lambda = c_G/f = (N/f)m \qquad [12]$$

known as the Rossby deformation radius.

The deformation radius is the natural horizontal scale for large-scale atmospheric dynamics. From eqn [12], it is the distance traveled by a gravity wave in the time (f^{-1}) required for Coriolis forces to deflect the velocity. It represents the spatial scale for adjustment of wind and pressure to geostrophic balance. This scale of adjustment increases with the static stability parameter N, and it decreases with rotation f.

The lowest-frequency class of large-scale dynamics is that of quasi-geostrophic (QG) dynamics for which '$\omega \ll f$' (*see* **Quasi-geostrophic Theory**). These motions are always near a state of geostrophic and hydrostatic balance, and are influenced strongly by static stability and the Earth's rotation. The QG form of the potential vorticity corresponding to eqn [10] has a variable part proportional to

$$q^* = \{\bar{N}^2\nabla^2 p' + f^2\,\partial^2 p'/\partial z^2\} \qquad [13]$$

The response of p' to thermal or vorticity forcing is determined by eqn [13], which is a three-dimensional Laplacian in coordinates that are stretched vertically according to N/f. It follows that point forcing yields an elliptically shaped response, with the major axis lying in the direction of least resistance. For example, large static stability of the stratosphere yields responses that are stretched horizontally and compressed vertically. For a given vertical scale, this property implies a horizontal influence distance equal to the deformation radius. For a given horizontal scale L, it implies a vertical influence distance called the Rossby depth, given by $H_R = (f/N)L$, so that

increasing the stability decreases the vertical coupling distance H_R.

Similar considerations may be applied to the QG 'omega equation' to distinguish the total response to various patterns of thermal and vorticity forcing, illustrating the crucial importance of static stability on large-scale dynamics through the ratio N/f. There are obvious global implications, since f is small at low latitudes. Two major regimes of large-scale atmospheric circulation are the result. For example, QG instability theory indicates that baroclinic wave and cyclone growth are possible only at mid–high latitudes. Hence the tropics are less variable, except in concentrated areas of moist convection (such as tropical cyclones) where conditionally unstable air lowers the effective ratio N/f. Similar arguments account for the difference among the atmospheric circulations of other planets.

Conclusions

Static stability acts through gravitational buoyancy forces to suppress vertical motions, and helps to control the weather systems and climate of the Earth. In the Earth's atmosphere, radiation and surface energy fluxes act to create three main categories of static stability.

1. *Strong stability*: The stratosphere is the most extensive example. Strong stability there encourages the vertical propagation of forced planetary waves through westerly winds regions, but it suppresses the growth of synoptic-scale circulations and convection.
2. *Weak static stability*: The troposphere is the atmosphere's dominant region of lesser, more variable static stability. As a result, instabilities may produce weather systems on a range of scales. For example, baroclinic wave circulations create variable weather in middle and high latitudes, and conditional instability may be realized as moist convection. Moist convection may be organized on the global scale (e.g., Hadley and Walker circulations), the synoptic scale (e.g., tropical cyclones), or the mesoscale (deep cumulus convection and severe weather). The static stability for dry processes may be strong enough to allow mesoscale mountain influences on the upper atmospheric wind, or to suppress small-scale shear instability which would otherwise produce clear air turbulence.
3. *Static instability*: The energy balance of the Earth system requires that the Earth's surface provides energy to the atmospheric boundary layer. This is often associated with static instability, dry convective motions, and sensible heating. Neutrally stable conditions are also very common, in which case turbulence transports latent energy away from the surface, enhancing the possibility of subsequent conditional instability.

In summary, the three regimes of static stability account for much of the variety of weather and climate. Ultimately, the various kinds of circulations feed back on the static stability field itself, leading to increased complexity of its space–time variability.

See also

Buoyancy and Buoyancy Waves: Theory. **Convective Storms:** Overview. **Dynamic Meteorology:** Overview. **Thermodynamics:** Moist (Unsaturated) Air; Saturated Adiabatic Processes. **Vorticity**.

Further Reading

Andrews DG, Holton JR and Leovy CB (1987) *Middle Atmosphere Dynamics*. Orlando, FL: Academic Press.

Chapman S and Lindzen RS (1970) *Atmospheric Tides. Thermal and Gravitational*. Dordrecht: Reidel.

Durran DR (1986) Another look at dowslope windstorms, Part 1. *Journal of Atmospheric Science* 43: 2527–2543.

Durran DR (1990) Mountain waves and downslope winds. In: Blumen W (ed.) *Atmospheric Processes over Complex Terrain*, pp. 59–82. Boston: American Meteorological Society.

Emanuel KA (1994) *Atmospheric Convection*. New York: Oxford University Press.

Gill AE (1982) *Atmosphere–Ocean Dynamics*. New York: Academic Press.

Holton JR (1992) *An Introduction to Dynamic Meteorology*, 3rd edn. New York: Academic Press.

Houze RA Jr (1993) *Cloud Dynamics*. San Diego: Academic Press.

Irbane JV and Godson WL (1981) *Atmospheric Thermodynamics*, 2nd edn. Dordrecht: Reidel.

Pedlosky J (1987) *Geophysical Fluid Dynamics*, 2nd edn. New York: Springer Verlag.

Scorer RS (1978) *Environmental Aerodynamics*. Chichester, UK: Ellis Horwood.

Sorbjan Z (1989) *Structure of the Atmospheric Boundary Layer*. Englewood Cliffs, NJ: Prentice-Hall.

Stull RB (1988) *An Introduction to Boundary Layer Meteorology*. Boston: Kluwer.

Tritton DJ (1996) *Physical Fluid Dynamics*, 2nd edn. New York: Oxford University Press.

Turner JS (1973) *Buoyancy Effects in Fluids*. London: Cambridge University Press.

Yih CS (1965) *Dynamics of Non-Homogeneous Fluids*. London: Macmillan.